2nd IEEE International Conference on Power and Energy (PECon 08), December 1-3, 2008, Johor Baharu, Malaysia

Reduction of Commutation Torque Ripple in a Brushless DC Motor Drive

S. S. Bharatkar[1], Raju Yanamshetti[1], D. Chatterjee[2] and A. K. Ganguli[2]

1 Research Scholar, Electrical Engineering Department, Jadavpur University, Kolkata – 700032, INDIA
E-mail: bharatkar_sachin@rediffmail.com.

2 Professor, Department of Electrical Engineering, Jadavpur University, Kolkata – 700032, INDIA
E-mail: dchatterjee@ee.jdvu.ac.in.

***Abstract*—This paper describes the reduction in torque ripple due to phase commutation of brushless dc motors. With two-phase 120^0 electrical conduction for the inverter connected to the conventional three-phase BLDC machine, the commutation torque ripple occurs at every 60 electrical degrees when a change over from one phase to another occurs. This effect increases the commutation time at higher speeds which increases the torque ripple. The torque ripple is reduced by changing the switching mode from 120^0 to a dual switching mode with 120^0 switching at lower speeds and 180^0 electrical for the inverter at higher speeds.**

***Keywords*—Brushless dc motor, current commutation, torque ripple, electric vehicle.**

I. INTRODUCTION

The recent progress in the area of magnetic materials and power semiconductors has improved the performance of brushless dc motors significantly. Its advantages are high power to weight ratio, high torque to current ratio, high dynamics-flexible control for variable speed operation, reduced maintenance due to absence of mechanical commutators (brushless-type) etc. These features have made brushless dc motors to be one of the best choices to replace conventional brush-type dc motors for many high performance applications. Brushless dc motors, having trapezoidal back emf waveform, when fed with rectangular stator current produces theoretically constant torque. However, in practice, torque ripple may exist due to several reasons e.g. toque ripple due to cogging, e.m.f. waveform imperfections, supply current ripple resulting from PWM inverters and from phase current commutation. It is desirable to minimize the torque ripple in a brushless dc (BLDC) drive to remove unacceptable speed ripple, vibration and acoustic noise. Thus in the past one decade, research effort was on to reduce such undesirable torque ripple in the machine. The cogging torque attenuation is mainly achieved by slot skewing or by changing the magnet's dimensions and positioning [1]. However, the torque ripple arising out from phase current commutation is one of the major problems for the BLDC drives.

In [2], it was shown that the commutation torque ripple might reach 50% of the average torque, but it could be eliminated at low speed by employing current control based on direct current sensing. In [2] and [3], it was concluded that it could not be compensated for by current chopping in the two-phase switching mode if the magnitude of the phase back-EMF is > 25% of the dc link voltage. In [4], two methods viz. overlapping conduction and PWM chopping were proposed, but because of first method torque ripple still results due to the difficulty in optimizing the overlap time. The second method significantly increases the system complexity and switching loss. In [5], commutation torque ripple was shown to result from the voltage between the neutral point of the inverter and the neutral point of the motor, which affects phase current during commutation. Adaptive torque-ripple control was proposed for BLDC motors in [6]. A commutation-torque-ripple reduction method for low cost application was presented in [7]. An alternative approach for minimizing torque ripple due to phase current commutation in a BLDC motor was developed in [8]. In [9], torque pulsations due to the interactions of the back-EMFs and currents and also due to commutation is reduced by employing torque controller. The application of direct toque control to a three- phase BLDC drive operating in 120^0 electrical conduction mode was proposed in [10]. The performance of a direct toque controlled BLDC drive has also been compared with that of a PWM current controlled drive, both with and without current shaping [11]. The estimation of the instantaneous electromagnetic torque was reported in [12]. The influence of PWM and cogging on the steady-state performance of a direct toque controlled BLDC drive was investigated in [13]. The commutation torque ripple minimization in direct toque controlled BLDC drive was presented in [14].

In this paper, an analytical study of commutation process is derived for inverters for both 120^0 and 180^0 conduction mode. It is seen that for 120^0 conduction mode, due to increase in commutation time at higher speeds, the torque ripple increases and hence will not be suitable at higher speeds. Also, for 180^0 conduction mode for the inverters, the commutation time increases at lower speeds and it is difficult to apply this switching mode at lower speeds. However, at higher speeds, this commutation time decreases to a lower value than that of 120^0 conduction mode and hence it is suitable to implement this switching strategy at these speeds. Therefore, a composite scheme is proposed where the 120^0 switching can be applied at lower speeds and at higher speeds the switching mode changes over to 180^0 mode. The commutation torque ripple is analyzed, based on the approach which was presented in [2], and is minimized by combining the conventional two-phase switching mode with a controllable three-phase switching mode during periods when the phase currents are being commutated. Its effectiveness is validated by both simulation and measurements.

II. Commutation Torque Ripple Analysis

In three-phase BLDC drive, idealized back-EMF and current waveforms are as shown in Fig. 1. A brushless dc motor drive consists of a permanent magnet machine fed by a current controlled inverter as shown in Fig. 2, where dc supply has been idealized.

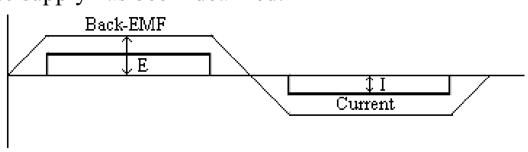

Fig. 1. Idealized Back-EMF and current waveforms in BLDC drive

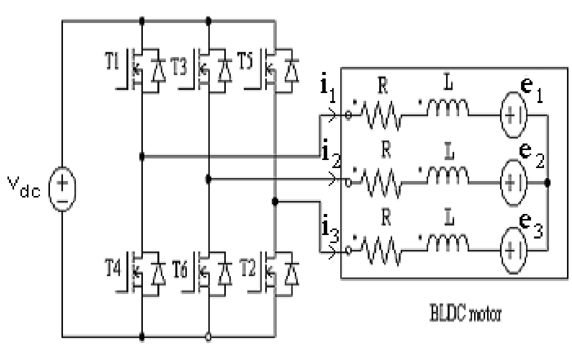

Fig. 2. PWM inverter and equivalent circuit of BLDC motor

The machine model and the conventions adopted for the study are also shown in Fig. 2. Assuming constant self and mutual inductances, the voltage equation of BLDC motor can be represented as (1).

$$\begin{bmatrix} v_1 \\ v_2 \\ v_3 \end{bmatrix} = \begin{pmatrix} R & 0 & 0 \\ 0 & R & 0 \\ 0 & 0 & R \end{pmatrix} \begin{bmatrix} i_1 \\ i_2 \\ i_3 \end{bmatrix} + \begin{pmatrix} L & 0 & 0 \\ 0 & L & 0 \\ 0 & 0 & L \end{pmatrix} \frac{d}{dt} \begin{bmatrix} i_1 \\ i_2 \\ i_3 \end{bmatrix} + \begin{bmatrix} e_1 \\ e_2 \\ e_3 \end{bmatrix} \quad (1)$$

Where R is phase resistance, i_1, i_2, i_3 are phase currents and e_1, e_2, e_3 are back-EMFs. The term $L = l - M$ with l is the self and M is the mutual inductance for the individual coils. The electromagnetic torque of the BLDC motor can be expressed as,

$$T = \frac{(e_1 i_1 + e_2 i_2 + e_3 i_3)}{\omega_m} \quad (2)$$

Where ω_m is the angular speed of the machine.

***Case-I: Two Phase (120^0) commutation mode*:**

The equation for 120^0 commutation for the inverter can be referred to Fig.2 and is described by the following equations [2].

$$\frac{di_1}{dt} = -\frac{(V+2E)}{3L} \quad (3)$$

$$\frac{di_2}{dt} = +\frac{2(V-E)}{3L} \quad (4)$$

$$\frac{di_3}{dt} = -\frac{(V-4E)}{3L} \quad (5)$$

$$i_1 = I - \frac{(V+2E)}{3L} t \quad (6)$$

$$i_2 = \frac{2(V-E)}{3L} t \quad (7)$$

$$i_3 = -I - \frac{(V-4E)}{3L} t \quad (8)$$

$$T = \frac{2E}{\omega} \left[I + \frac{(V-4E)}{3L} t \right] \quad (9)$$

Here i_1, i_2, i_3 are the phase currents. V is the supply dc voltage and E is per phase back EMF. If, V = 4E, the machine torque remains constant where as, for V < 4E, the torque decreases and for V > 4E, the torque increases.

***Case-II: Proposed three Phase (180^0) commutation mode*:**

In order to show torque ripple due to the supply, ideal trapezoidal emf's e_1, e_2, e_3 are considered. For analysis the transistors T5, T6, T1 are assumed to conduct initially. Then the transistor T5 is switched off and before T2 turns on diode D2 will provide the current path. At the end of commutation period, the transistors T6, T1, T2 will be on making changeover of current. The corresponding equivalent circuit is shown in Fig.3. (a) and (b).

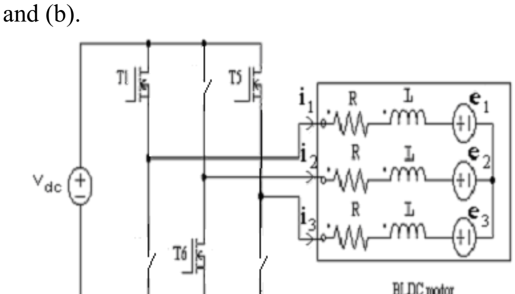

(a)

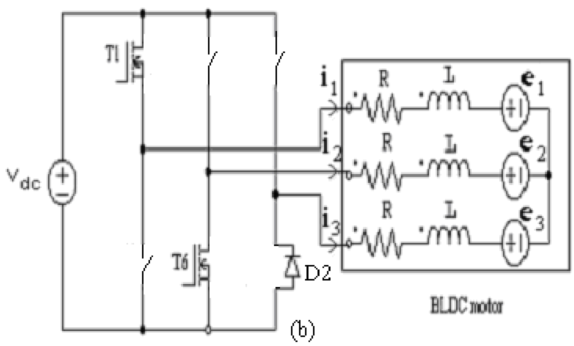

Fig.3. Commutation sequence (a) before commutation (b) commutation with two switches and one diode conducting.

For the sequence of Fig. 3(b), the current derivatives are given by,

$$\frac{di_1}{dt} = -\frac{(V+2E)}{3L} \tag{10}$$

$$\frac{di_2}{dt} = \frac{(V-4E)}{3L} \tag{11}$$

$$\frac{di_3}{dt} = 2\frac{(V-E)}{3L} \tag{12}$$

Taking the beginning of the commutation as the time origin, the phase currents are given by

$$i_1 = \frac{I}{2} - \frac{(V+2E)}{3L}t \tag{13}$$

$$i_2 = -I + \frac{(V-4E)}{3L}t \tag{14}$$

$$i_3 = \frac{I}{2} + 2\frac{(V-E)}{3L}t \tag{15}$$

From the above equations, it is possible to determine the commutation sequence's duration and the condition for three cases to occur. The commutation time is assumed to be t_f.

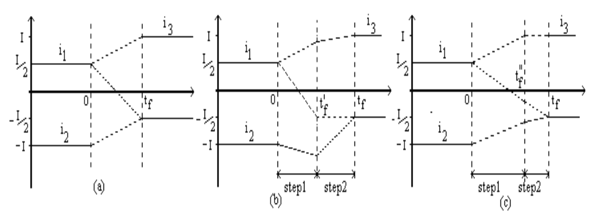

Fig. 4. Current variation during current commutation (a) V=10E (b) V>10E (c) V<10E.

Case a: Referring to Fig. 4(a), $i_1(t_f) = -\frac{I}{2}$ then, the commutation time t_f can be calculated from (13) as

$$t_f = \frac{3LI}{(V+2E)} \tag{16}$$

But it is also known that $i_2(t_f) = -\frac{I}{2}$; then, from (14)

$$t_f = \frac{3LI}{2(V-4E)} \tag{17}$$

Thus, from equations (16) and (17),

$$V = 10E \tag{18}$$

For a constant voltage V at the input of the inverter, this condition corresponds to a given speed.

The commutation duration is given by,

$$t_f = \frac{LI}{4E} \tag{19}$$

Case b: In this case, i_1 reaches from I/2 to –I/2 earlier than t_f. The commutation is made in two sequences as shown in Fig. 4. (b). The first sequence, defined by the time that current i_1 takes to reverse which is characterized by the circuit of Fig.3 (b). The duration of this step is given from (13) by

$$t_f' = \frac{3LI}{(V+2E)} \tag{20}$$

At the end of this sequence, current i_2 is given from (14) by

$$i_2(t_f') = -I\frac{6E}{V+2E} \tag{21}$$

The condition for having case 'b' is given by $i_2(t_f') < -\frac{I}{2}$, that is from (21)

$$V \rangle 10E \tag{22}$$

The total duration of the commutation is given by,

$$t_f = \frac{9LI(V-6E)}{2(V+2E)(V-4E)} \tag{23}$$

When the duration of commutation t_f becomes larger than, $\pi/3\omega$, the current in the machine winding does not reach the reference current I, and then, it is no longer controlled. This limit depends on the value of the current and on the speed.

Case c: In this case, i_1 reaches from I/2 to –I/2 later than t_f considered in case a. The commutation time t_f'' can be calculated by assuming that the phase current i_2 will become –I/2 at the end of commutation as shown in Fig. 4 (c). Thus, from (14),

$$t_f'' = \frac{3LI}{2(V-4E)} \tag{24}$$

At the instant t_f'' , the current i_1 is given from (13)

$$i_1(t_f'') = -\frac{6E}{2(V-4E)}I \tag{25}$$

Thus, the condition for having $i_1(t_f'') > -\frac{I}{2}$ is given by

$$V \langle 10E \tag{26}$$

After analysis, total duration t_f of the commutation can be obtained as

$$t_f = \frac{3LI}{(V+2E)} \qquad (27)$$

Torque during commutation:

a. 120^0 conduction mode [2]:

The relative torque ripple for V<4E is given by

$$\Delta T = \frac{(V-4E)}{(V+2E)} \text{ (pu)} \qquad (28)$$

And the relative torque ripples for V>4E is given by

$$\Delta T = \frac{(V-4E)}{2(V-E)} \text{ (pu)} \qquad (29)$$

b. Proposed 180^0 conduction mode:

From the general expression of torque given in (2), the machine torque can be written as,

$$T = \frac{\left(Ei_1 + Ei_2 + Ei_3\right)}{\omega_m}$$

As, $i_1 + i_2 + i_3 = 0$ giving $i_1 + i_3 = -i_2$ in this case then,

$$T = -\frac{2E}{\omega_m} i_2 \qquad (30)$$

This result shows that the torque is proportional to the current not directly involved in the commutation.
Replacing i_2 by the expression of (14) becomes

$$T = \frac{2E}{\omega}\left[I - \frac{(V-4E)}{3L} t_f\right] \qquad (31)$$

From (30) and (31), it can be seen that when V = 10E (case a) torque remains constant, with V > 10E (case b) torque decreases and with V < 10E (case c) torque increases.
To evaluate the torque ripple amplitude during commutation, it is only necessary to calculate its value at the end of the first step, that is, for V > 10E (case b)

$$T(t_f') = \frac{2E}{\omega}\left[I - \frac{(V-4E)}{3L} t_f'\right] \qquad (32)$$

The relative torque ripple is given by,

$$\Delta T = \frac{T(t_f') - T}{T}$$

And for the present analysis, the relative torque ripple is obtained as,

$$\Delta T = -\frac{(V-4E)}{(V+2E)} \text{ (pu)} \qquad (33)$$

For V=10E, $\Delta T = -0.5\,pu$

Again, for V<10E, the $T\,(t_f'')$ is given by

$$T(t_f'') = \frac{2E}{\omega}\left[I - \frac{(V-4E)}{3L} t_f''\right] \qquad (34)$$

The relative commutation torque ripple is computed after replacing t_f'' from (24) and is given by,

$$\Delta T = -0.5(pu) \qquad (35)$$

Which means that it remains constant at –0.5 pu value.

III. Simulation Results

The relative torque ripple and commutation time t_f is plotted for both 120 and 180 degree conduction mode in Fig. 5 (a) and (b).

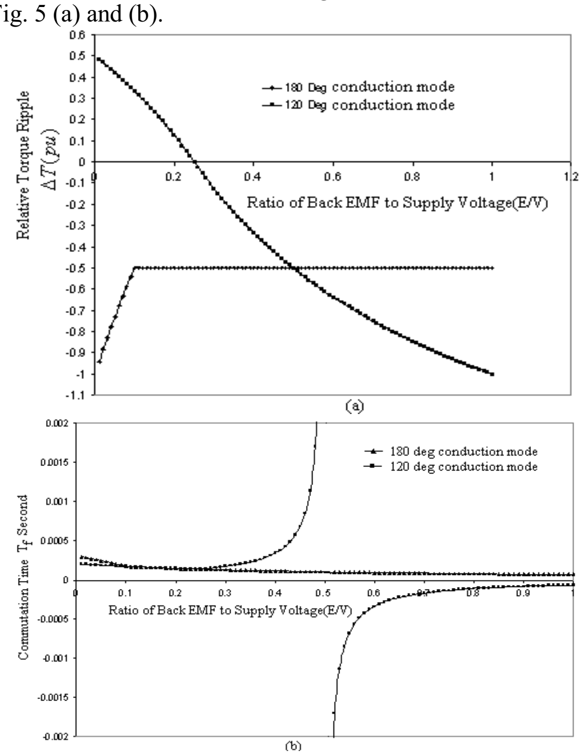

Fig.5. (a) Relative torque ripple amplitude and (b) The duration of commutation time

The relative torque ripple and the duration of the commutation calculated from the above equations for a given machine can be synthesized as shown in Fig.5. It is seen from Fig. 5(b) that for 120^0 conduction mode, at higher speeds, the commutation time increases and hence will not be suitable at higher speeds. For 180^0 conduction mode for the inverters, the commutation time increases at lower speeds and also from Fig. 5(a) it is revealed that torque ripple is more thus it is difficult to apply this switching mode at lower speeds. However, at higher speeds, this commutation time decreases to a lower value than that of 120^0 conduction mode and hence it is suitable to implement this switching strategy at these speeds. The relative torque ripples remains within $\pm$50% in both the cases except some higher values at lower speeds for 180^0 conduction mode.

IV. Experimental Results

Experiments performed with a motor having specifications given in table-1 along with a MOSFET based PWM inverter. The core of the driving system is DSP TMS320F2407A. The main advantage of this chip are, increased system reliability and cost reduction of the overall system. The output pulses from the TMS320F2407A DSP are not capable of driving the MOSFETs with higher ratings. Hence isolated device drivers are used. Six driver circuits are used to drive the MOSFETs. The experimental setup of BLDC drive is as shown in Fig. 6. At lower and higher speeds the plot of torque with respect to time is given in Fig. 7 for 180 degree conduction mode. The plots validated the theoretical formulations. The torque with respect to time and current with respect to time for speed reference of 400 rpm is shown in Fig. 8 and Fig. 9 respectively. Similarly, the plot of current with respect to time and torque with respect to time for speed reference of 3000 rpm is as shown in Fig. 10 and Fig. 11 respectively.

Fig.6. Experimental setup of BLDC drive.

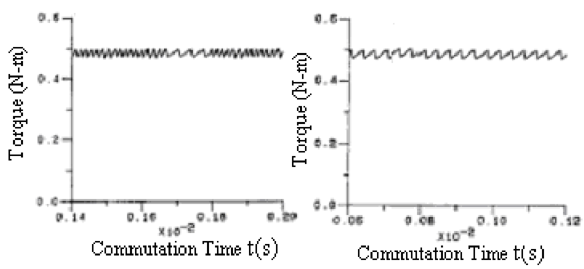

Fig.7. Torque Vs. time for 180^0 conduction mode with speed reference of 3000 rpm and 400 rpm.

TABLE I
MACHINE SPECIFICATIONS

Rated Power	550W
Rated voltage	48V DC
Rated Speed	3000 rpm
Rated Current	11.2 Amps
Resistance	2.5 Ω
Inductance	11.2 mH
Emf Constant	0.016 V/rpm

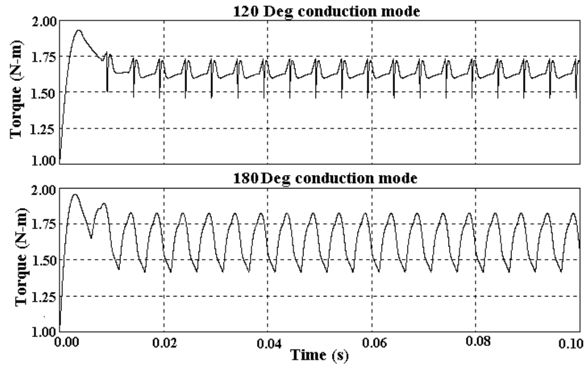

Fig.8. Torque Vs. time for speed reference of 400 rpm.

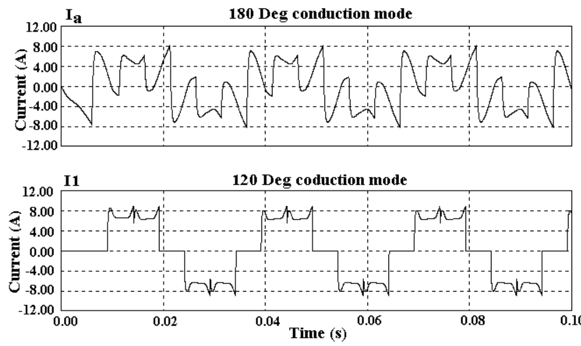

Fig.9. Current Vs. time for speed reference of 400 rpm.

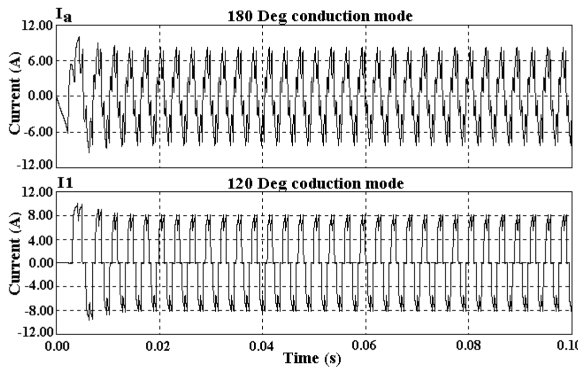

Fig.10. Current Vs. time for speed reference of 3000 rpm.

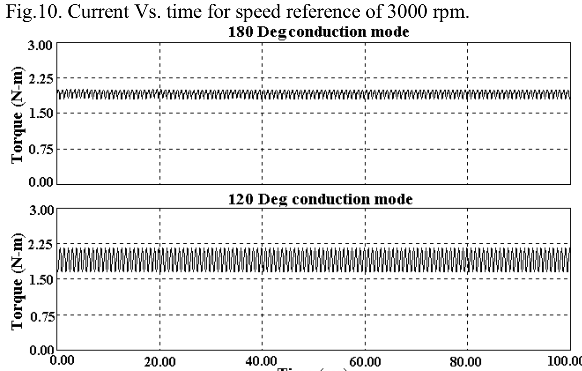

Fig.11. Torque Vs. time for speed reference of 3000 rpm.

V. Conclusion

This paper has presented an analytical study of torque ripple comparison due to commutation of phase currents in a brushless dc motor for both 120^0 and 180^0

conduction modes. The results have been validated by simulation and experimental verification. In three-phase switching mode at high speeds the torque ripple and losses are minimized and therefore the efficiency of the machine is increased. But the same cannot be achieved at low speed in this mode. On the other hand, the 120^0 situation is exactly opposite. Thus a composite switching scheme is proposed for satisfactory operation of the machine at all speeds. The effectiveness of the method is validated by suitable experiments.

VI. REFERENCES

[1] T. Li, and G. Slemon, "Reduction of cogging torque in permanent magnet motors," *IEEE Trans. on Magnetics*, vol.24, no.6, pp.2901-2903, Nov. 1988.

[2] R. Carlson, M. Lajoie-Mazenc, and J.C.D.S. Fagundes, "Analysis of torque ripple due to phase commutation in brushless DC machines," *IEEE Trans. Ind. Appl.*, vol.28, no.3, pp. 632-638, May/Jun. 1992.

[3] H. Tan, "Controllability analysis of torque ripple due to phase commutation in brushless DC motors," in *Proc. 5th int. conf. Elect. Mach. And Syst.*, Aug. 18-20, 2001, vol.2, pp. 1317-1322.

[4] Y. Murai, Y. Kawase, K. Ohashi, K. Nagatake and K. Okuyama, "Torque ripple improvement for brushless DC miniature motors," *IEEE Trans. Ind. Appl.*, vol.25, no.3, pp. 441-450, May/Jun. 1989.

[5] C.S. Berendsen, G. Champenois, and A. Bolopion, "Commutation strategies for brushless DC motors: Influence on instant torque," *IEEE Trans. Power Electron.*, vol.8, no.2, pp. 231-236, Apr.1993.

[6] Y. Sozer and D.A. Torrey, "Adaptive torque ripple control of permanent magnet brushless DC motors," *Proc. 13th Annu. Appl. Power Electron. Conf. and Expo.*, Feb. 15-19, 1998, vol.1, pp. 86-92.

[7] D.K. Kim, K.W. Lee, and B.I. Kwon, "Torque ripple reduction method in a sensorless drive for the BLDC motor," *Korean IEE Int. Elect. Mach. Energy Convers. Syst.*, vol. 4-B, no.4, pp.196-200, 2004.

[8] T.S. Kim, S.C. Ahn, and D.S. Hyun, "A new current control algorithm for torque ripple reduction of BLDC motors," *Proc. 27th Annu. Conf. IEEE Ind. Electron. Soc.*, Nov.29-Dec.2, 2001, vol.2, pp.1521-1526.

[9] S.J. Kang and S.K. Sul, "Direct torque control of brushless DC motor with non-ideal trapezoidal back-EMF," *IEEE Trans. Power Electron.*, vol.10, no.6, pp.796-802, Nov.1995.

[10] Y. Liu, Z.Q. Zhu, and D. Howe, "Direct torque control of brushless DC drives with reduced torque ripple," *IEEE Trans. Ind. Appl.*, vol.41, no.2, pp.599-608, Mar./Apr.2005.

[11] Z.Q. Zhu, Y. Liu, and D. Howe, "Comparison of performance of brushless DC drives under direct torque control and PWM current control," *Korean IEE Int. Elect. Mach. nergy Convers. Syst*., vol. 5-B, no.4, pp.337-342, 2005.

[12] Y. Liu, Z.Q. Zhu, and D. Howe, "Instantaneous torque estimation in sensorless direct torque controlled brushless DC motors," *IEEE Trans. Ind. Appl.*, vol.42, no.5, pp.1275-1283, Sept./Oct.2006.

[13] Z.Q. Zhu, Y. Liu, and D. Howe, "Steady-state dynamic performance of a direct torque controlled PM brushless DC drive accounting for influence of PWM chopping and cogging torque," in *Proc. IEE Int. Conf. Power Electron., Mach. And Drives*, Dublin, Ireland, Apr. 4-6, 2006, pp.556-560.

[14] Y. Liu, Z.Q. Zhu, and D. Howe, "Commutation torque ripple minimization in direct torque controlled PM brushless DC drives," *IEEE Trans. Ind. Appl.*, vol.43, no.4, pp. 1012 -1021, July/Aug.2007.

[15] T.J.E. Miller, *Brushless Permanent Magnet and Reluctance Motor Drives*. Oxford: Clarendon, 1989.

[16] R. Krishnan, *Electric Motor Drives: Modeling, Analysis, and Control*, Prentice Hall, New Jersey, 2001.